CrossMark

A broad-band polarization-insensitive absorber with a wide angle range metamaterial for thermo-photovoltaic conversion

Fathi Bendelala[1] · Ali Cheknane[1] · Hikmat S. Hilal[2]

Abstract A new absorber design using metamaterials for thermo photovoltaic applications is simulated here. Conventional absorbents normally have narrow band-widths and/or sensitive-polarization. Alternatively, the present study shows the possibility to find an infrared absorber structure with optimal characteristics involving a metal-dielectric. A combination of two resonators, circular cavity in a square metallic patch, laid on a dielectric substrate is proposed here. With this design, the results show that wide-band absorption can be achieved. The absorption bandwidth can be widened from 57.2 to 95.4 THz, with absorption efficiency higher than 90%. This structure design is polarization-insensitive to incident electromagnetic wave angles. These new features make the new absorber potentially useful in thermo-photovoltaic conversion applications.

Keywords Thermo-photovoltaic · Absorption · Polarization-insensitive · Metamaterials

1 Introduction

Metamaterials (MTMs) have several optical properties that make them suitable for microwave and optical frequency applications. MTMs have unique electromagnetic properties not widely encountered in nature, such as negative permittivity, negative permeability, and negative refractive index (Cai and Shalaev 2010). Theoretically, the electromagnetic properties of MTMs have been reported to be negative by several groups (Ziolkowski and Auzanneau 1997; Caloz et al. 2001). Experimental studies have confirmed this phenomenon and applications derived from it. Examples are phase compensation and electrically small resonators (Engheta 2002), negative angles of refraction (Engheta 2002;

✉ Ali Cheknane
  cheknanali@yahoo.com; a.cheknane@lagh-univ.dz

1 Laboratoire des semiconducteurs et matériaux fonctionnels, Université Amar Telidji de Laghouat, Bd des Martyrs BP37G, 03000 Laghouat, Algeria

2 SSERL, Chemistry Department, An-Najah National University, Nablus, Palestine

Foteinopoulou et al. 2003), sub-wavelength waveguides with lateral dimension below diffraction limits (Alù and Engheta 2004), backward-wave antennas (Grbic and Eleftheriades 2002), Cerenkov radiation (Lu et al. 2008), photon tunneling (Zhang and Fu 2002).

Recently, MTMs have become a focal area for research. The MTM absorbers have many applications including, miniature antenna (Zhang et al. 2014), energy harvesting (Wang et al. 2015), invisible cloak (Iwaszczuk et al. 2012), and sensor detecting (Meng et al. 2012). Moreover, some MTM absorbers are tunable (Cheng et al. 2016; Han and Lee 2016).Different MTM absorber designs have been utilized in different frequency ranges, including microwaves (Du et al. 2014; Bhattacharyya et al. 2015), far-infrared (Feng et al. 2014; Jiang et al. 2011), terahertz (Peng et al. 2015; Gao et al. 2015), and optical frequencies (Duan et al. 2014; Wu et al. 2014). Most of these applications have one perfect absorption band frequency. Therefore, the absorption bandwidth is very narrow. To increase the absorption bandwidth, attempts were made using different techniques. Qin et al. (Feng et al. 2012) suggested an absorber in the long-wavelength infrared region by utilizing the frequency dispersion of MTM surface. An absorption bandwidth ranging from 21 to 44 THz can thus be achieved with an absorption rate more than 97%. Chen et al. (2015a) used the high-impedance surface to design a broadband absorber in the microwave region, and showed absorption ranging from 3.65 to 13.93 GHz, with absorption efficiency higher than 90%. Furthermore, alternative structures were also proposed. Double-circle rings loaded with lumped resistances are reported (Chen et al. 2015b).Three-dimensional structures for enhancing the width-band absorption were also suggested (She et al. 2015).

The infrared radiation range is popularly known as heat radiation, which is commonly divided into three regions. The far-infrared, from 300 GHz to 30 THz (1–10 μm) corresponds to very low temperatures (-80.15 to -270.15 °C). The mid-infrared, from 37 to 120 THz (10–2.5 μm), corresponds to medium temperatures (89–693 °C). The near-infrared, from 120 to 400 THz (2500–750 nm), corresponds to higher temperatures (693–3591 °C) (Morozhenko 2012). The mid-infrared (thermal infrared) is mostly used in thermo-photovoltaic (TPV) conversion.

This work describes a new MTM absorber with special features. A broad-band absorption range (56.2–95.4 THz) with absorption efficiency higher than 90%, with insensitive polarization is described. The maximal absorption efficiency can reach 99.9%. Moreover, the system may accommodate radiations from wide angles.

2 Materials and methods

When infrared radiations strike TPV cells, three different behaviors may occur, reflection, absorption and transmission. The performance of a TVP cell structure is mainly affected by these scattering phenomena, where the scattering parameters can be defined as (Rafangura and Sabah 2015):

$$S_{11} = \frac{\int_{port1} ((E_c - E_1)E_1^*)dA_1}{\int_{port1} (E_1 \cdot E_1^*)dA_1} \tag{1}$$
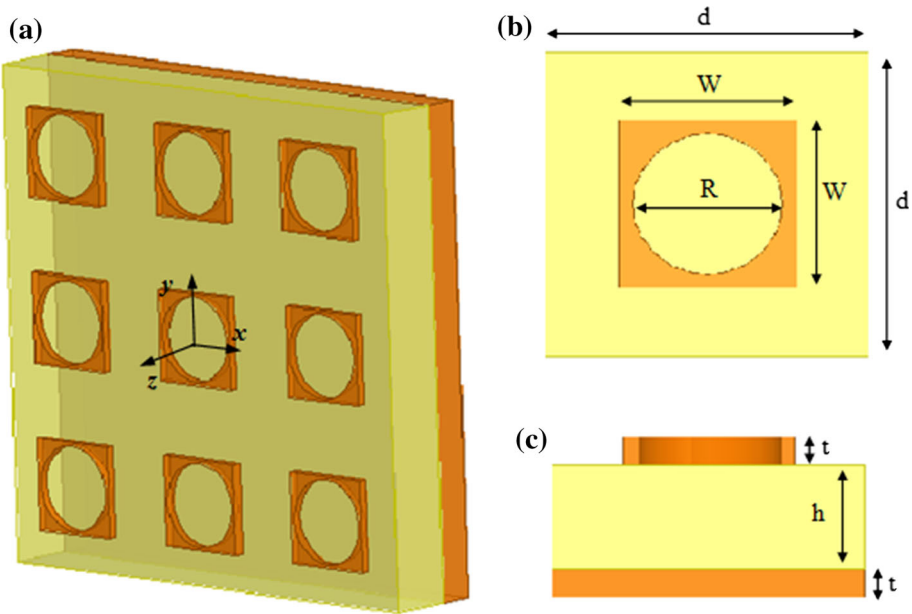
(a)

(b)

(c)

Fig. 1 Design of MTM absorber structure from different views; **a** array of periodic unit cells **b** typical front unit cell view; **c** typical bottom unit cell view

$$S_{21} = \frac{\int_{port2} (E_c \cdot E_2^*) dA_2}{\int_{port2} (E_2 \cdot E_2^*) dA_2} \tag{2}$$

E_1 and E_2 are the electric patterns on the first and the second excitation ports, port 1 and port 2, respectively. It is also possible to calculate the S-parameters from the power flow through the two ports in terms of the power flow.

$$S_{11}(\omega) = \frac{\sqrt{Power\ reflected\ from\ port_1}}{\sqrt{Power\ incident\ on\ port_1}} \tag{3}$$

$$S_{21}(\omega) = \frac{\sqrt{Power\ transmitted\ to\ port_2}}{\sqrt{Power\ incident\ on\ port_1}} \tag{4}$$

$$A(\omega) = 1 - |S_{11}(\omega)|^2 - |S_{21}(\omega)|^2 \tag{5}$$

$A(\omega)$ is the absorption, $S_{11}(\omega)$ and $S_{21}(\omega)$ are the scattering matrix parameters which are directly related with the reflected and transmitted waves.

In the study of optical field problems, the selection of appropriate numerical simulation software to be used for that particular issue is a vital step. Thus, the decision on the numerical software needs careful attention to the type of optical wave understudy. The methods which are widely used for numerical analyses of optical problems, Finite Element Method (FEM), and Finite Difference Time Domain technique (FDTD), are chosen here (Cai and Shalaev 2010).
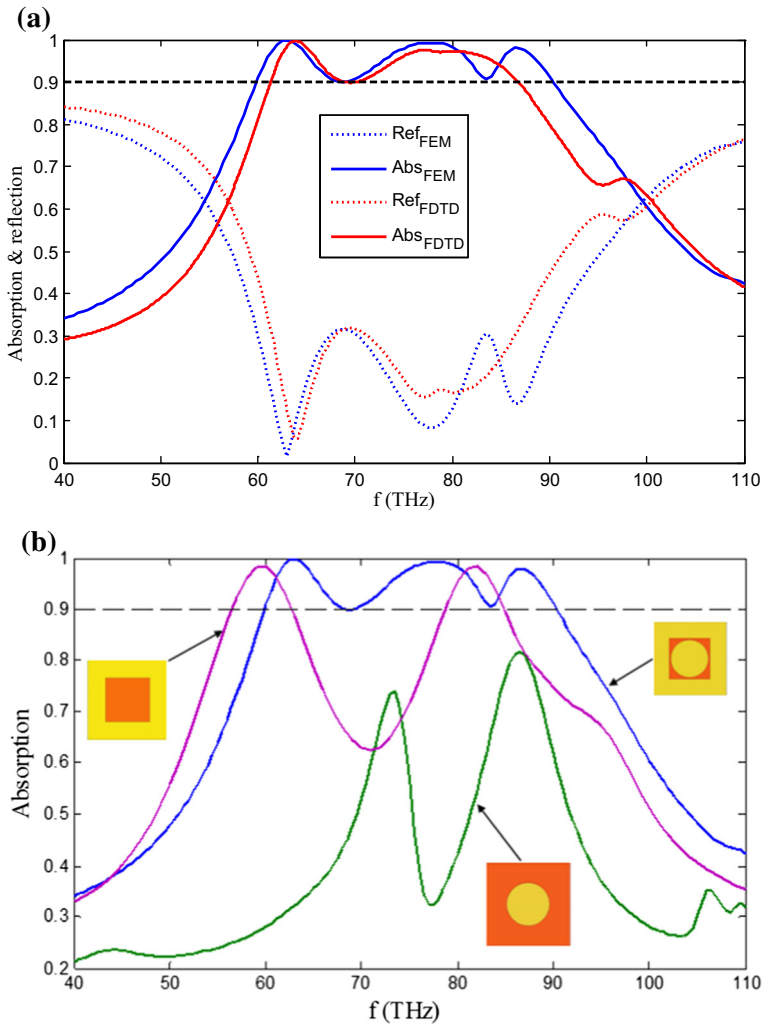
Fig. 2 Simulated spectra for **a** the designed MTM absorber, **b** metal structure effect

3 Results and discussion

The new MTM absorber unit cell is shown in Fig. 1 with different views. The unit cell involvesa circular cavity in a square metal plateresonator on the top, a metal ground plane on the bottom, and a dielectric material in between. The geometric parameters of this absorber are given as, $h = 420$ nm, $W = 2150$ nm, $R = 2000$ nm, $d = 3900$ nm, $t = 200$ nm, the dielectric spacer is SiN with a relative permittivity $\varepsilon = 5.28 + i0.23$. Tungsten, with an electrical conductivity 182×10^6 S/m, is used for this design. The dielectric function of metallic shapes (ground plane and squares resonator) is described by the Drude model, which can be expressed in terahertz domain as,
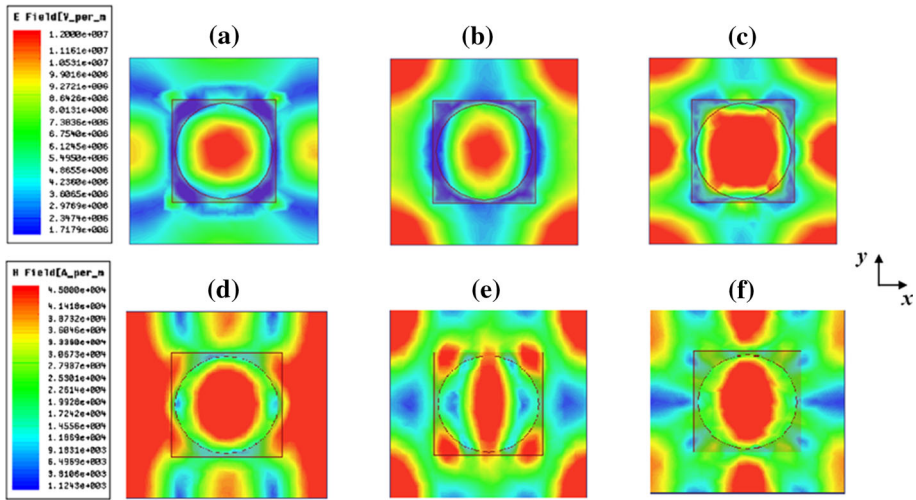
Fig. 3 Distribution of electric field |E| for TE polarization at different frequencies **a** 63 THz, **b** 78 THz, **c** 89.5 THz. Distribution of magnetic field |H| for TM polarization at, **a** 63 THz, **b** 78 THz, **c** 89.5 THz

$$\varepsilon(\omega) = 1 - \frac{\omega_p^2}{\omega \cdot (\omega - i\omega_c)} \tag{6}$$

The plasma frequency ω_P is 1448 THz and the collision frequency ω_c is 13 THz (Ordal et al. 1983). The simulated results are based on two different approaches, finite element method by the HFSS software, and finite difference time domain by the CST software. Thus, care is taken to keep high stability and validity of simulation results in THz frequency. In the x and y directions, the unit cell boundary conditions were applied assuming perfect E, and perfect H, respectively. Open space boundary conditions were used in the z-direction. It is assumed that the transmission coefficient $S_{21}(\omega) = 0$ if the thickness of the metal is greater than the skin depth, so the expression (5) can be simplified as.

$$A(\omega) = 1 - |S_{11}(\omega)|^2 \tag{7}$$

Figure 2a shows the simulated absorption and reflection spectra of the designed MTM. The absorption spectra show three resonance points, $f_1 = 63$ THz, $f_2 = 78$ THz and $f_3 = 89.5$ THz with absorption coefficients of 99.9, 99.3, and 98.1%, respectively. The absorption bandwidth can achieve a high bandwidth of 38.2 THz, where the absorptivity is larger than 90%. This structure gives polarization-insensitive absorber and has the same absorption for transverse electric (TE) and transverse magnetic (TM) polarized waves.

From Fig. 2b it can be seen that a simple square metal, or single cavity element, cannot achieve high absorption especially at high frequencies. However, if these two structures are combined, in the same absorber resonator design, a strong interaction between these two elements is observed. As the electromagnetic field is confined inside the dielectric, more electromagnetic field energy is absorbed by the dielectric, and the cavity causes higher absorbance for electromagnetic energy.

This absorption is a result of an impedance adaptation between the effective impedance of MTM structure $Z_{eff}(\omega)$ and free space impedance $Z_0(\omega)$ (Lee et al. 2016):
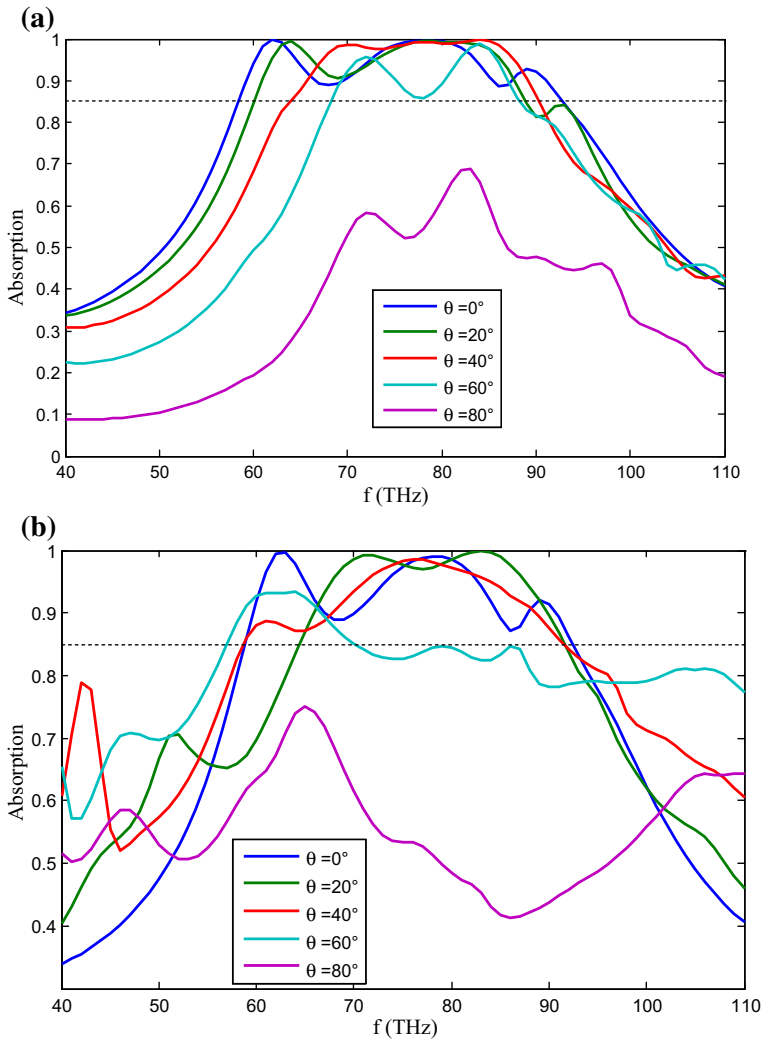
(a)

(b)

Fig. 4 Absorption effect of different angles of incidence; **a** TE polarization wave; **b** TM polarization wave

$$Z_{eff}(\omega) = Z_0(\omega) \tag{8}$$

$$Z_0(\omega) = \sqrt{\frac{\mu_0}{\varepsilon_0}} \tag{9}$$

$$Z_{eff}(\omega) = \sqrt{\frac{\mu_{eff}(\omega)}{\varepsilon_{eff}(\omega)}} \tag{10}$$
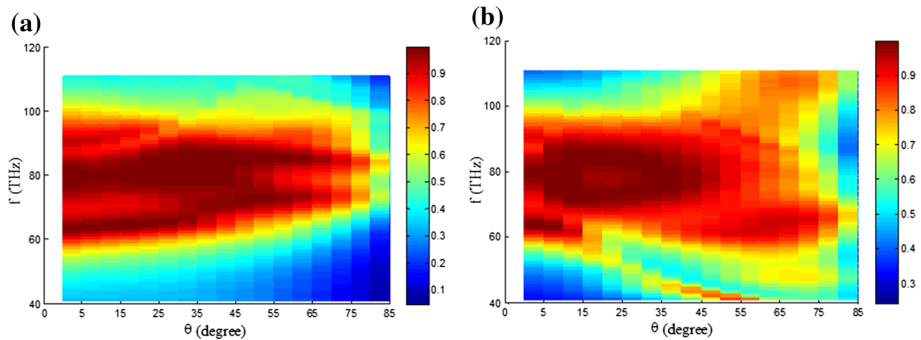
(a)

(b)

Fig. 5 Diagram of dispersion for absorbed energy by different incidence angles for **a** TE polarization wave, and **b** TM polarization wave

This happens by carefully toiling MTM structure geometric parameters which leads to alteration of both effective electric permittivity $\varepsilon_{eff}(\omega)$ and effective magnetic permeability $\mu_{eff}(\omega)$ of the MTM structure.

To better understand the absorption mechanism of the new MTM absorber, the distributions of the electric field and the magnetic field in the dielectric layer are shown in Fig. 3. Firstly, for the TE mode polarization, Fig. 3a illustrates the three electric field absorption zones at 63 THz, aligned with the x direction. At the frequency 78 THz, five absorption areas can be seen, four in the corner of the unit cell, and a fifth in the center, are shown in Fig. 3b. Secondly, for the TM polarization, the transverse magnetic absorption mechanism is quite complicated compared to transverse electric field, in this case the magnetic field vector is everywhere transverse, and the electric field of the TM modes is mostly a small axial component. The distributions of magnetic field indicate that the large charges are accumulated at the edge of the metallic shapes, as well as in the center of circular cavity. The magnetic field absorption at the resonance frequency for the TM polarization is illustrated in Fig. 3d–f. It can be observed that the absorbed electromagnetic field is strongly focused on several zones of dielectric during all absorption frequencies for TE or TM polarization waves.

In TPV applications, it is preferable to have MTM absorbers with a wide angle of incidence. In the present structure, the results for different incidence angles are shown in Fig. 4. As for TE polarization, the largest incidence angle can reach 70° when the minimal absorption rate is more than 85%. For TM polarization, the largest incidence angle can be 60°.

Furthermore, the absorption is simulated as a function of frequency and incident angle in Fig. 5 to examine the angle dependence of this broadband absorber. As seen in Fig. 5a, b, the broadband absorption is insensitive to the incident angle for TE and TM polarizations, and the minimal absorption magnitude from 58 to 90 THz is larger than 0.85 for angles up to 60° for a different polarizations. Therefore, the present broadband absorber can operate in a wide-angle range.

The mechanism of the broadband absorption may explain the influence of geometric parameters on the frequencies and the bandwidth. As shown in Fig. 6a, the size of the period d is important to tune the frequencies of the absorber. This is because the variation in the period d can significantly influence the interaction of adjacent cells, and consequently tune the bandwidth and absorption rate of the absorber. Figure 6b, which is a plot of absorption versus length of the square metallic patch, shows that the absorption rate
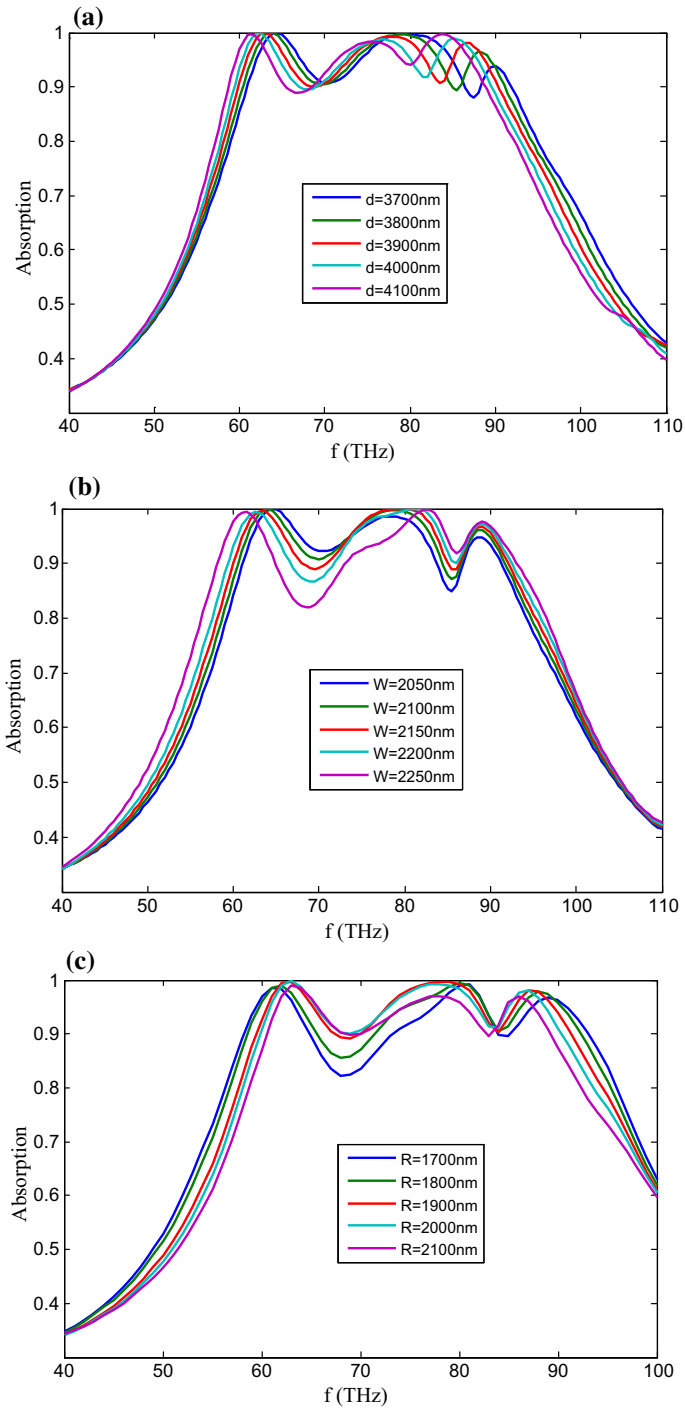
Fig. 6 Dependence of the absorption spectra on the **a** period of unit cell, **b** length of square metallic patch, **c** diameter of circular cavity

gradually decreases with the increase of the square patch length. A random shift in frequency resonance can also be seen. The diameter of the circular cavity R gives the same effect with the period d, as shown in Fig. 6c.

4 Conclusion

This work describes a new highly efficient MTM absorber, compared to earlier ones. A circular cavity in square metallic patch is used here, as alternative to bulky layers or multi form of resonators in the same structure. Thus the square patch and the circular cavity have strong mutual interaction causing higher absorption for electromagnetic waves with broad wavelength range. The study showed that we can reach a maximal absorption rate of 99.9%. Due to the symmetry of this design, it is polarization-insensitive for different incident angles. Moreover this structure is useful for wide angle of incidence, up to 70° and 60°, for TE and TM polarization waves, respectively.

References

Alù, A., Engheta, N.: Guided modes in a waveguide filled with a pair of single negative (SNG), double-negative (DNG), and/or double-positive (DPS) layers. IEEE Trans. Microw. Theory Tech. **MTT-52**(1), 199–210 (2004)

Bhattacharyya, S., Ghosh, S., Chaurasiya, D., Srivastava, K.V.: Bandwidth-enhanced dual-band dual-layer polarization-independent ultra-thin metamaterial absorber. Appl. Phys. A **118**, 207–215 (2015)

Cai, W., Shalaev, V.: Optical Metamaterials Fundamentals and Applications. Springer, New York (2010)

Caloz, C., Chang, C.-C., Itoh, T.: Full-wave verification of the fundamental properties of left-handed materials in waveguide configurations. J. Appl. Phys. **90**(11), 5483–5486 (2001)

Chen, J.F., Hu, Z., Wang, G., Huang, X., Wang, S., Hu, X., Liu, M.: High-impedance surface-based broadband absorbers with interference theory. IEEE Trans. Antennas Propag. **63**, 4367–4373 (2015a)

Chen, J., Huang, X., Zerihun, G., Hu, Z., Wang, S., Wang, G., Hu, X., Liu, M.: Polarization-independent, thin, broadband metamaterial absorber using double-circle rings loaded with lumped resistances. J. Electron. Mater. **44**, 4269–4274 (2015b)

Cheng, Y., Mao, X.S., Wu, C., Wu, L., Gong, R.Z.: Infrared non-planar plasmonic perfect absorber for enhanced sensitive refractive index sensing. Opt. Mater. **53**, 195–200 (2016)

Du, Q., Zeng, Z., Xiang, D., Lv, T., Zhang, G., Yang, H.: Stable high absorption metamaterial for wide angle incidence of terahertz wave. J. Mod. Opt. **61**, 621–625 (2014)

Duan, X., Chen, S., Liu, W., Cheng, H., Li, Z., Tian, J.: Polarization-insensitive and wide-angle broadband nearly perfect absorber by tunable planar metamaterials in the visible regime. J. Opt. **16**, 125107 (2014). https://doi.org/10.1088/2040-8978/16/12/125107

Engheta, N.: An idea for thin subwavelength cavity resonators using metamaterials with negative permittivity and permeability. IEEE Antennas Wirel. Propag. Lett. **1**, 10–13 (2002)

Feng, Q., Pu, M., Hu, C., Luo, X.: Engineering the dispersion of metamaterial surface for broadband infrared absorption. Opt. Lett. **37**, 2122–2135 (2012)

Feng, R., Qiu, J., Cao, Y., Liu, L., Ding, W., Chen, L.: Omnidirectional and polarization insensitive nearly perfect absorber in one dimensional meta-structure. Appl. Phys. Lett. **105**, 181102 (2014). https://doi.org/10.1063/1.4901073

Foteinopoulou, S., Economou, E.N., Soukoulis, C.M.: Refraction in media with a negative refractive index. Phys. Rev. Lett. **90**(10), 107402 (2003). https://doi.org/10.1103/PhysRevLett.90.107402

Gao, R., Zongcheng, X., Ding, C., Liang, W., Yao, J.: Graphene metamaterial for multiband and broadband terahertz absorber. Opt. Commun. **356**, 400–404 (2015)

Grbic, A.A., Eleftheriades, G.V.: Experimental verification of backward-wave radiation from a negative refractive index metamaterial. J. Appl. Phys. **92**, 5930–5935 (2002)

Han, S.H., Lee, B.J.: Electromagnetic resonance modes on a two-dimensional tandem grating and its application for broadband absorption in the visible spectrum. Opt. Express **24**(2), A202–A214 (2016). https://doi.org/10.1364/OE.24.00A202

Iwaszczuk, K., Strikwerda, A.C., Fan, K., Zhang, X., Averitt, R.D., Jepsen, P.U.: Flexible metamaterial-absorbersfor stealth applications at terahertz frequencies. Opt. Express **20**, 635–643 (2012)

Jiang, Z.H., Yun, S., Toor, F., Werner, D.H., Mayer, T.S.: Conformal dual-band near-perfectly absorbing mid- infrared metamaterial coating. Nano **5**, 4641–4647 (2011)

Lee, Y.P., Rhee, J.Y., Yoo, Y.J., Kim, K.W.: Metamaterials for Perfect Absorption. Springer, New York (2016)

Lu, J., Grzegorczyk, T.M., Zhang, Y., Pacheco Jr., J., Wu, B.-I., Kong, J.A., Chen, M.: Cerenkov radiation in materials with negative permittivity and permeability. Opt. Express **11**, 723–734 (2008)

Meng, F.Y., Wu, Q., Erni, D., Wu, K., Lee, J.C.: Polarization-independent metamaterial analog of electromagnetically induced transparency for a refractive-index-based sensor. IEEE. Trans. Microw. Theory Tech. **60**, 3013–3022 (2012)

Morozhenko, V.: Infrared Radiation. In Tech (2012). ISBN: 978-953-51-0060-7

Ordal, M.A., Long, L.L., Bell, R.J., Bell, S.E., Bell, R.R., Alexander Jr., R.W., Ward, C.A.: Optical properties of the metals Al Co, Cu, Au, Fe, Pb, Ni, Pd, Pt, Ag, Ti, and W in the infrared and far infrared. Appl. Opt. **22**, 1099–1119 (1983)

Peng, Y., Zang, X.F., Zhu, Y.M., Shi, C., Chen, L., Cai, B., Zhuang, S.L.: Ultra-broadband terahertz perfect absorber by exciting multi-order diffractions in a double-layered grating structure. Opt. Express **23**, 2032–2039 (2015)

Rafangura, P., Sabah, C.: Dual-band perfect metamaterial absorber for solar cell applications. Vacuum **120**, 68–74 (2015)

She, Y., Pang, Y., Wang, J., Ma, H., Pei, Z., Shaobo, Q.: Origami-inspired metamaterial absorbers for improving the larger-incident angle absorption. Appl. Phys. **48**, 445008 (2015). https://doi.org/10.1088/0022-3727/48/44/445008

Wang, H., Sivan, P.V., Mitchell, A., Rosengarten, G., Phelan, P., Wang, L.: Highly efficient selective metamaterial absorber for high-temperature solar thermal energy harvesting. Sol. Energy Mater. Sol. Cells **137**, 235–242 (2015)

Wu, J., Zhou, C., Yu, J., Cao, H., Li, S., Jia, W.: Polarization-independent absorber based on a cascaded metal- dielectric grating structure. IEEE Photonics Technol. Lett. **26**, 949–952 (2014)

Zhang, Z.M., Fu, C.J.: Unusual photon tunneling in the presence of a layer with negative refractive index. Appl. Phys. Lett. **80**, 1097–1099 (2002)

Zhang, H., Cao, X.-Y., Gao, J., Yang, H.-H., Yang, Q.: A novel dual-band metamaterial absorber and its application for microstrip antenna. Prog. Electromag. Res. Lett. **44**, 35–41 (2014)

Ziolkowski, R.W., Auzanneau, F.: Passive artificial molecule realizations of dielectric materials. J. Appl. Phys. **82**(7), 3195–3198 (1997)